In-Situ Study of Dynamics of Refractive Index Changes in Silicon Devices Induced by UV-light Irradiation

Jiaqi Wang, Zhiwei Wei, Huabin Qiu, Zhengkun Xing, Yuzhi Chen, Youfu Geng, Yu Du, Xuejin Li, and Zhenzhou Cheng

***Abstract*—Silicon photonics has been studied in various areas by providing small-footprint, high-performance, and mass-producible optoelectronic components integrated on a chip. For the photonic packaging, ultraviolet (UV) curing techniques have been widely utilized. Meanwhile, silica cladding absorption to UV light could alter its refractive index (RI), affecting the optical testing of silicon devices during or after the device packaging. Therefore, it is significant to characterize the dynamics of RI changes induced by UV-light irradiation. However, the in-situ characterization of such devices is seldom explored. Here, we studied the influence of UV-light irradiation on silicon photonic devices by probing resonant wavelength shifts of a racetrack microring resonator. Specifically, we studied the temporary variation of the resonant wavelength and its recovery time under different UV-light exposure durations. Experimental results show that with a UV energy of 21 J/cm^2, the resonator had a maximum resonant wavelength shift of 0.31 nm, corresponding to an effective RI change of 0.0009 and recovering time of 95 minutes. Based on the experimental results, we compressively analyzed and compared RI changes induced by plasmon dispersion effect, thermal optical effect and photon-induced silica densification effect. Our study is expected to provide useful guidelines for in-situ silicon photonic testing and packaging.**

***Index Terms*—Silicon photonics, photonic packing, microring resonator, integrated optics, waveguide, grating coupler.**

Manuscript received May 4, 2022; revised May 23, 2022; accepted June 5, 2022. Date of publication June 10, 2022; date of current version June 17, 2022. This work was supported in part by the National Natural Science Foundation of China under Grants 62161160335, 62175179, 61805164, 61805175, and 61775149, in part by the Natural Science Foundation of Guangdong under Grant 2021A1515011680, and in part by the Science and Technology Plan Project of Shenzhen under Grants JCYJ20190808120801661 and JCYJ20190808145207437. *(Corresponding authors: Zhenzhou Cheng; Xuejin Li.)*

Jiaqi Wang, Zhiwei Wei, Huabin Qiu, Yuzhi Chen, Youfu Geng, Yu Du, and Xuejin Li are with the College of Physics and Optoelectronic Engineering, Shenzhen University, Shenzhen 518060, China, and also with the Shenzhen Key Laboratory of Sensor Technology, Shenzhen 518060, China (e-mail: jqwang@szu.edu.cn; 2070456095@email.szu.edu.cn; 2070456092@email.szu.edu.cn; chenyuzhi@szu.edu.cn; gengyf@szu.edu.cn; duyu@szu.edu.cn; lixuejin@szu.edu.cn).

Zhengkun Xing and Zhenzhou Cheng are with the School of Precision Instrument and Optoelectronics Engineering, Tianjin University, Tianjin 300072, China, and also with the Key Laboratory of Optoelectronics Information Technology, Ministry of Education, Tianjin 300072, China (e-mail: xingzhengkun@tju.edu.cn; zhenzhoucheng@tju.edu.cn).

Digital Object Identifier 10.1109/JPHOT.2022.3181352

I. Introduction

SILICON photonic integrated circuits (PICs) are considered as a promising platform for optical communications, interconnects, and ranging [1], [2] with the high-density integration of a variety of optoelectronic components on a chip, namely, power splitters [3], [4], arrayed waveguide gratings [5], [6], Mach-Zehnder interferometers [7], [8], microring resonators (MRRs) [9], [10], electro-optical modulators [11], [12] and photodetectors [13]. In the development of the fiber-to-chip packaging process, laser welding with metals [14], soldering with metals/inorganic materials [15], and bonding with ultraviolet (UV) cured or thermally cured epoxies have been widely used [16]. Among the above techniques, the bonding with UV curable epoxies has the advantages of room-temperature operation, low cost, and high flexibility of fiber-to-chip alignment. To date, the fiber-to-chip interfaces includes in-plane couplers (e.g., inverted tapers [17], [18]) and out-of-plane couplers (e.g., diffractive gratings [19], [20]).After aligning optical fibers and silicon waveguides, UV curable epoxies are utilized to adhere the optical fibers to the optical components [21].

On the other hand, silica cladding absorption to UV light could alter its refractive index (RI), affecting the optical testing of silicon devices during or after the fiber-to-chip packaging process. According to a previous study, the RI variation could be in the range from 10^{-5} to the order of 10^{-3} depending on the UV light energy as well as exposure time [22]. Moreover, the RI change could be a reversible process and the recovery conditions, such as the heating temperature and duration, vary with the constituents of the silica film [22]. The RI variation inevitably influences the characterization of other photonic devices on the same chip, namely, resonators with high-quality factors. Therefore, it is significant to study the dynamics of RI changes induced by UV-light irradiation. However, the in-situ characterization of the UV-light-irradiation-induced RI variation in silicon devices is seldom explored, to the best of our knowledge.

Herein, we experimentally studied the effect of UV-light irradiation on the RI change of the silicon devices with silica cladding by probing resonant wavelength shifts of a racetrack MRR. We studied the variation of the resonant wavelength and its recovery time (defined as the time it takes for the resonant wavelength to go back to the initial measurement under room temperature without UV light irradiation) under different UV

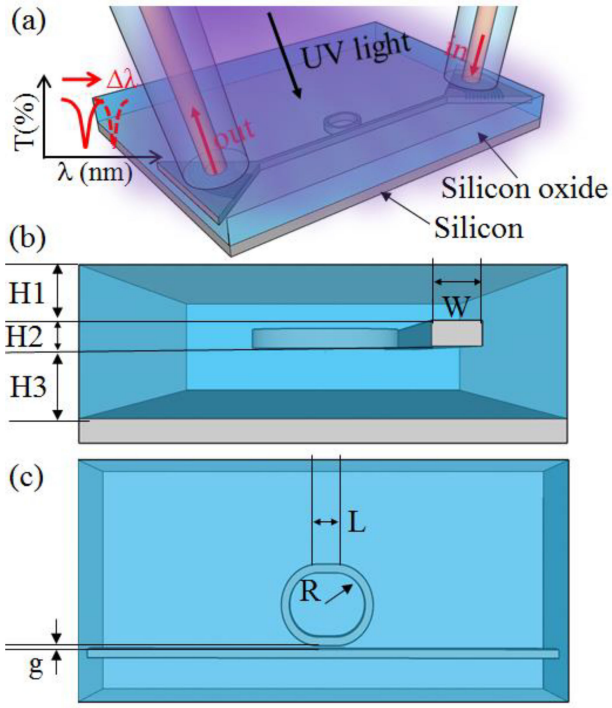

Fig. 1. Schematic of the designed racetrack MRR. (a) Three-dimensional view of the racetrack MRR coupled by using the focusing grating couplers. (b) Cross-section view of the racetrack MRR. (c) Top view of the racetrack MRR.

light exposure durations. Experimental results show that with a UV energy of 21 J/cm^2, the MRR had a maximum resonant wavelength shift of 0.31 nm, corresponding to an effective RI change of 0.0009 and recovering time of 95 minutes. Our study can provide useful guidelines for the research and development of silicon PICs.

II. Design and Fabrication of the Silicon Devices

The silicon devices were designed based on a silicon-on-insulator wafer with a 220-nm thick silicon layer and 3-μm thick buried oxide (BOX) substrate. Focusing grating couplers with a period of 600 nm and filling factor of 0.5 were designed to couple TE-mode light between optical fibers and silicon waveguide devices, as shown in Fig. 1(a). There is 1-μm thick silica fabricated by using plasma-enhanced chemical vapor deposition as a top cladding layer (H1), as shown in Fig. 1(b). The top view of the device is shown in Fig. 1(c). The width of the waveguide is 450 nm for the single-mode operation. The radius (R) of the racetrack MRR is 10 μm. The gap (g) between the microring and bus waveguide is 250 nm. We simulated the cross-coupling power ratio of the racetrack MRR with varying the directional coupler length (L) by using a BeamPRO simulator. The cross-coupling power ratio increases from 0 to 25% with the length of the directional coupler (in the range from 0 to 20 μm). The strip waveguide propagation loss is 2 dB/cm, according to the process standard of the multi-project wafer (MPW) foundry. Therefore, to meet the critical coupling condition, we chose L as 2.5 μm to reach the cross-coupling power of 3%.

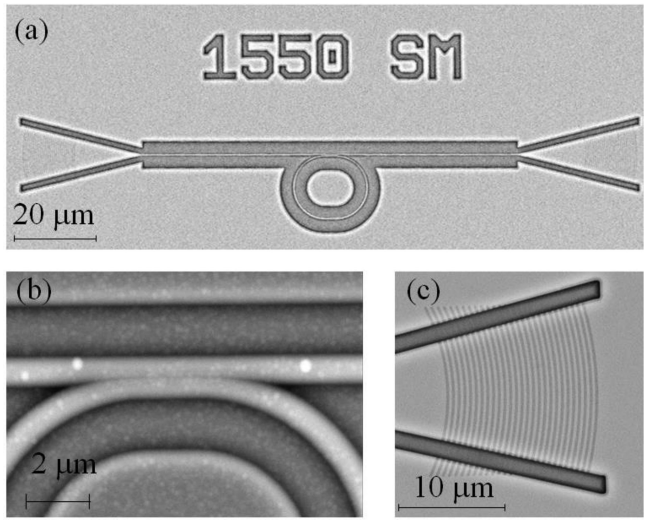

Fig. 2. SEM images of the fabricated devices. (a) The racetrack MRR coupled by using a pair of the focusing grating couplers. (b) Directional coupler of the racetrack MRR. (c) Zoom-in image of the focusing grating coupler.

Based on the designs, we fabricated the silicon devices by using a standard multi-project wafer service. The scanning electron microscope (SEM) image of the fabricated racetrack MRR is shown in Fig. 2(a), which is coupled by using a pair of the focusing grating couplers. The zoom-in images of the gap between the bus waveguide and racetrack MRR, as well as the focusing grating coupler, are shown in Fig. 2(b) and (c), respectively. According to the SEM image, the gap and coupling length agree well with our design.

III. Device Measurement and Result Discussion

First, we measured the transmission spectrum of the racetrack MRR by using a tunable laser (HP 8168) and optical power meter (HP 81531A). The input optical power was set as -10 dBm to avoid possible nonlinear absorption losses. The coupling efficiency of the focusing grating coupler was measured from the same design but connected by a single-mode waveguide with a short length of 150 μm. As shown in Fig. 3(a), the focusing grating coupler has a peak coupling efficiency of -5.14 dB and 1-dB bandwidth of 26 nm at the center wavelength of 1557.24 nm. The coupling profile was used to normalize the transmission spectrum of the racetrack MRR for different UV-light irradiation and temperature conditions in the experiment. As shown in Fig. 3(b), the free spectral range (FSR) of the racetrack MRR is 8.23 nm which agrees well with our design. Moreover, according to the Lorentz fitting of the transmission spectrum around the wavelength of 1555.75 nm, the racetrack MRR has a Q factor of 28000 with an extinction ratio of 19.8 dB.

Second, we studied the UV-light-irradiation-induced RI change in the silica-cladding silicon device. A 365-nm-wavelength UV light source with a power density of 5 mW/cm^2, which was characterized by using an intensity meter (OAI 308), was used in the experiment. The 365-nm-wavelength light sources are commonly used in epoxy curing. The device was placed on a thermal electric cooler (TEC) controlled by

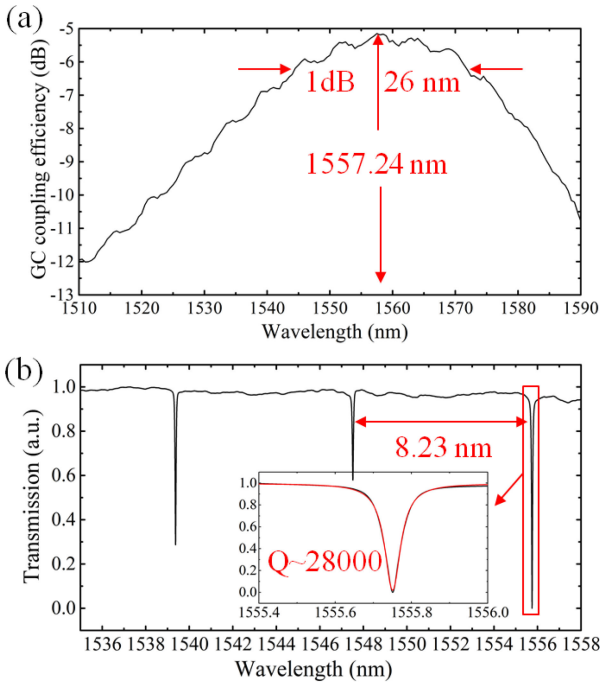

Fig. 3. Measurement results of the fabricated devices. (a) Coupling profile of the focusing grating coupler. (b) Transmission spectrum of the racetrack MRR. The inset is the zoom-in image of the transmission measurement at the wavelength of around 1555.75 nm, indicating the Q factor of ~28000.

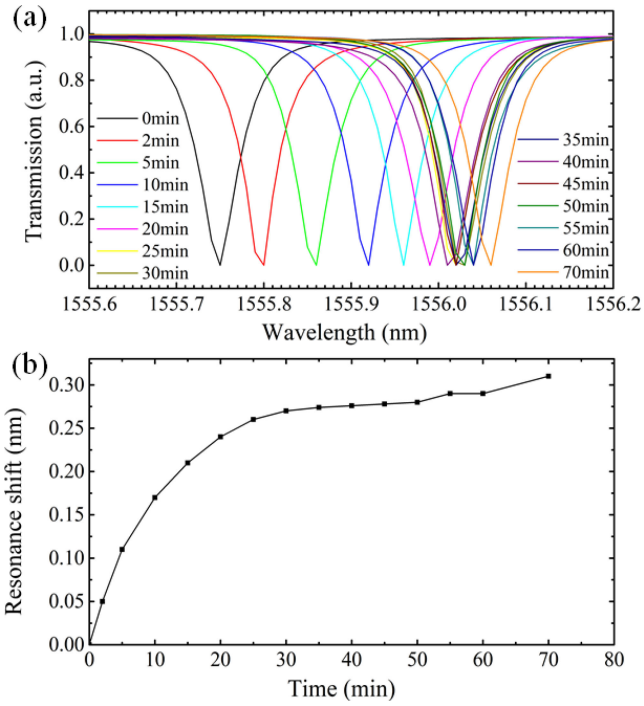

Fig. 4. Influence of the UV-light irradiation on the racetrack MRR. (a) Transmission spectrum of the racetrack MRR as a function of UV-light irradiation duration. (b) Resonant wavelength shift as a function of the UV-light irradiation exposure duration.

a semiconductor laser diode driver to tune the temperature. Meanwhile, the chip temperature was monitored by using a thermistor. The TEC was used to keep the temperature constant during the UV-light-irradiation experiment. We measured the transmission spectra of the racetrack MRR under different irradiation durations from 2 minutes to 70 minutes, as shown in Fig. 4(a). With the UV-light irradiation, the resonance at the wavelength of 1555.75 nm had a redshift, indicating that the effective RI of the waveguide mode increased. With increasing the duration of the UV-light irradiation, the shift of resonance firstly grew fast and then slower, as shown in Fig. 4(b). With the maximum irradiation duration of 70 minutes, which corresponds to the UV-light energy used in the fiber-to-chip bonding process [21] (calculated in the range from 10 J/cm^2 to 600 J/cm^2), the resonance shift can be as large as 0.31 nm. It is worthwhile to note that the full-width half maximum of the resonant curve kept almost consistent during the UV-light irradiation, indicating that neglectable free carriers were generated during the UV-light irradiation experiment.

Besides, we also analyzed the dynamic behavior of the resonance shift after the UV-light irradiation, as shown in Fig. 5. When the UV light source was turned off, the resonance first had a sharp blue shift in a short time and then gradually decreased to the initial value. For the case of the 2-minutes UV-light irradiation, the redshift of resonance is 0.05 nm, as shown in Figs. 4(a) and 5(a). After the 2-minutes UV-light irradiation, it took 50 minutes for the resonance to decrease from 1555.81 nm to 1555.75 nm, as shown in Fig. 5(a). The recovery time is much longer than that induced by the thermal optical effect which was measured in the range from 1 to 170 μs [23]. Moreover,

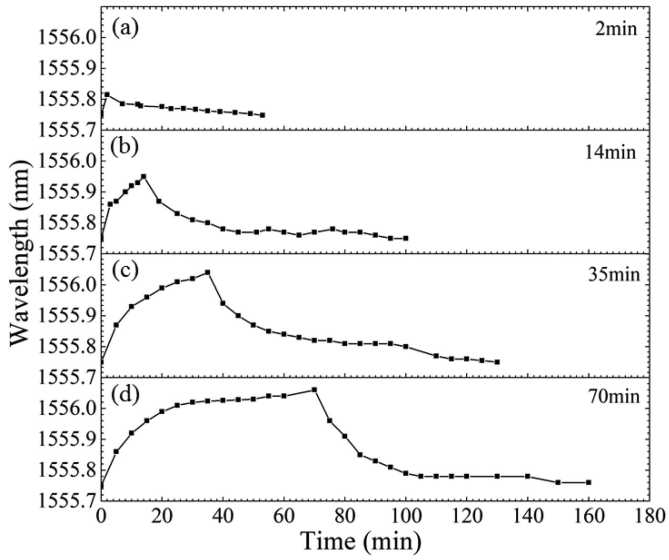

Fig. 5. Dynamics of the resonant wavelength shift of the racetrack MRR. (a)-(d) Resonant wavelength monitoring with the UV exposure times of 2, 14, 35, and 70 minutes.

larger UV-light irradiation energy can lead to a longer recovery time. For the 35 minutes and 70 minutes UV-light irradiations, which are comparable with the commonly used UV light energy for the epoxy curing [21], it took 90 minutes and 95 minutes for the racetrack MRR to shift back to the initial resonant wavelength. It is worth noting that the UV-light irradiation-induced RI change could be possibly attributed to the optical

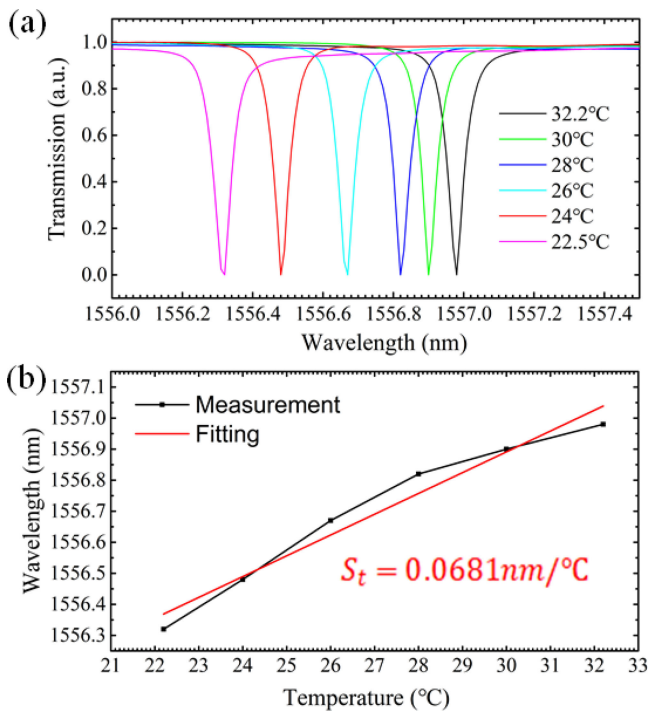

Fig. 6. Thermal tuning of the resonant wavelength of the racetrack MRR. (a) Measured transmission spectra of the racetrack MRR under different temperatures. (b) Resonant wavelength shift as a function of temperature.

absorption of silicon waveguide core and cladding materials. The photoexcited carrier density of silicon could be deduced from the Drude model and estimated as 8.8×10^{12} cm^{-3}[24]. Then the following expression can be used to estimate the RI change of silicon [25],

$$\Delta n = -[8.8 \times 10^{-22} \times \Delta n_e + 8.5 \times 10^{-18} \times (\Delta n_h)^{0.8}] \quad (1)$$

where Δn_e and Δn_h are the change of free-electron and free-hole carrier density, respectively. The calculated RI change was 1.41×10^{-7}, which could hardly change the resonance of the racetrack MRR. The limited free carrier generation agrees well the measurement of the unchanged full-wave half maximum of the resonant curve in Fig. 4(a). Therefore, the resonant wavelength change could be caused by the RI change of the silica cladding caused by the photon-induced silica densification effect [26], [27], which has been demonstrated to be a reversible process.

Finally, we compared the UV-light irradiation-induced resonance shift with that introduced by the thermal-optical effect. We measured the transmission spectrum of the racetrack MRR at different temperatures, as shown in Fig. 6(a). The resonance increases linearly with the chip temperature, due to the positive thermal-optic coefficients of silicon (1.8×10^{-4}/°C) and silicon oxide (9.6×10^{-6}/°C) [28]. From the linear fitting of Fig. 6(b), the temperature sensitivity of the resonance (St) is 0.0681 nm/°C. We simulated the effective RI of the waveguide mode as a function of the temperature. The obtained temperature sensitivity is 0.0002 ERIU/°C, where ERIU is the effective RI unit. The effective RI sensitivity of the resonance was calculated as 340.5 nm/ERIU. As shown in Fig. 4(b), when the UV light irradiation duration was 70 minutes, the redshift of the resonance is 0.31 nm, corresponding to an effective RI change of 9×10^{-4}. Then, we fixed the RI of silicon and changed the RI of silicon oxide cladding to simulate the effective RI of the waveguide mode. In the simulation, we increased the RI of the silicon oxide by 0.002868 to reach the same RI change. The shift of the resonance induced by the 70-minute UV-light irradiation is comparable with a temperature change of 5 °C but suffering from a much longer covering time.

IV. Conclusion

In summary, we experimentally explored dynamic RI changes in silicon devices introduced by the UV-light irradiation by monitoring the resonance shift of the racetrack MRR. Due to the material densification effect of the silica cladding, the RI increased, leading to the redshift of the resonance. Then, the resonance gradually recovered when the UV light was turned off. The dependence of the recovery time on the UV irradiation energy was characterized. Our study provides useful instructions for the PIC package process.

References

[1] L. Li *et al.*, "A fully-integrated flexible photonic platform for chip-to-chip optical interconnects," *J. Lightw. Technol.*, vol. 31, no. 24, pp. 4080–4086, Dec. 2013.
[2] S. Zheng *et al.*, "Silicon-based four-mode division multiplexing for chip-scale optical data transmission in the 2 μm waveband," *Photon. Res.*, vol. 7, no. 9, pp. 1030–1035, Sep. 2019.
[3] J. T. Kim, "Silicon optical modulators based on tunable plasmonic directional couplers," *IEEE J. Sel. Topics Quantum Electron.*, vol. 21, no. 4, pp. 184–191, Jul. 2015.
[4] H. Sattari, A. Y. Takabayashi, Y. Zhang, P. Verheyen, W. Bogaerts, and N. Quack, "Compact broadband suspended silicon photonic directional coupler," *Opt. Lett.*, vol. 45, no. 11, pp. 2997–3000, Jun. 2020.
[5] B. Chen *et al.*, "Unidirectional large-scale waveguide grating with uniform radiation for optical phased array," *Opt. Exp.*, vol. 29, no. 13, pp. 20995–21010, Jun. 2021.
[6] Q. Fang *et al.*, "Folded silicon-photonics arrayed waveguide grating integrated with loop-mirror reflectors," *IEEE Photon. J.*, vol. 10, no. 4, Aug. 2018, Art. no. 4900508.
[7] Q. Li, J.-H. Han, C. P. Ho, S. Takagi, and M. Takenaka, "Ultra-power-efficient 2 × 2 Si Mach-Zehnder interferometer optical switch based on III-V/Si hybrid MOS phase shifter," *Opt. Exp.*, vol. 26, no. 26, pp. 35003–35012, Dec. 2018.
[8] Y. Dattner and O. Yadid-Pecht, "Analysis of the effective refractive index of silicon waveguides through the constructive and destructive interference in a Mach–Zehnder interferometer," *IEEE Photon. J.*, vol. 3, no. 6, pp. 1123–1132, Dec. 2011.
[9] M. M. Milosevic *et al.*, "Ion implantation of germanium into silicon for critical coupling control of racetrack resonators," *J. Lightw. Technol.*, vol. 38, no. 7, pp. 1865–1873, Apr. 2020.
[10] Ó. G. López, D. Van Thourhout, D. Lasaosa, M. López-Amo, R. Baets, and M. Galarza, "Vertically coupled microring resonators using one epitaxial growth step and single-side lithography," *Opt. Exp.*, vol. 23, no. 4, pp. 5317–5326, Feb. 2015.
[11] F. Qiu *et al.*, "Athermal hybrid silicon/polymer ring resonator electro-optic modulator," *ACS Photon.*, vol. 3, no. 5, pp. 780–783, Apr. 2016.
[12] H. Yan *et al.*, "One-dimensional photonic crystal slot waveguide for silicon-organic hybrid electro-optic modulators," *Opt. Lett.*, vol. 41, no. 23, pp. 5466–5469, Feb. 2016.
[13] T. Komljenovic *et al.*, "Heterogeneous silicon photonic integrated circuits," *J. Lightw. Technol.*, vol. 34, no. 1, pp. 20–35, Jan. 2016.
[14] J. H. Song, H. N. J. Fernando, B. Roycroft, B. Corbett, and F. H. Peters, "Practical design of lensed fibers for semiconductor laser packaging using laser welding technique," *J. Lightw. Technol.*, vol. 27, no. 11, pp. 1533–1539, Apr. 2009.

[15] H. Lu *et al.*, "Flip-chip integration of tilted VCSELs onto a silicon photonic integrated circuit," *Opt. Exp.*, vol. 24, no. 15, pp. 16258–16266, Jul. 2016.
[16] Z. Zhang, G. Xiao, J. Liu, and C. P. Grover, "Coupling fibers to planar waveguides using a high-temperature epoxy," *Fiber Integr. Opt.*, vol. 22, no. 6, pp. 357–371, Jun. 2003.
[17] M. Papes *et al.*, "Fiber-chip edge coupler with large mode size for silicon photonic wire waveguides," *Opt. Exp.*, vol. 24, no. 5, pp. 5026–5038, Mar. 2016.
[18] M. Tokushima, H. Kawashima, T. Horikawa, and K. Kurata, "Post-Integrated dual-core large-end spot-size converter with Si vertical taper for fiber butt-coupling to Si-photonics chip," *J. Lightw. Technol.*, vol. 36, no. 20, pp. 4783–4791, Oct. 2018.
[19] Z. Cheng and H. K. Tsang, "Experimental demonstration of polarization-insensitive air-cladding grating couplers for silicon-on-insulator waveguides," *Opt. Lett.*, vol. 39, no. 7, pp. 2206–2209, Apr. 2014.
[20] T.-H. Xiao *et al.*, "Mid-infrared high-Q germanium microring resonator," *Opt. Lett.*, vol. 43, no. 12, pp. 2885–2888, Jun. 2018.
[21] G. Bond *et al.*, "Direct attachment of optical fibers to photonic integrated circuits with in situ UV curing," in *Proc. Conf. Lasers Electro-Opt.*, San Jose, CA, USA, 2021, Paper JW1A.29.
[22] M. Douay *et al.*, "Densification involved in the UV-based photosensitivity of silica glasses and optical fibers," *J. Lightw. Technol.*, vol. 15, no. 8, pp. 1329–1342, Aug. 1997.
[23] P. Dong *et al.*, "Thermally tunable silicon racetrack resonators with ultralow tuning power," *Opt. Exp.*, vol. 18, no. 19, pp. 20298–20304, Sep. 2010.
[24] K. Salek, K. Takayama, I. Kawayama, H. Murakami, and M. Tonouchi, "Evaluation of surface carrier recombination of optically excited silicon using terahertz time-domain spectroscopy," *Terahertz Sci. Technol.*, vol. 7, no. 2, pp. 100–107, Mar. 2014.
[25] G. T. Reed, G. Mashanovich, F. Y. Gardes, and D. J. Thomson, "Silicon optical modulators," *Nature Photon.*, vol. 4, no. 8, pp. 518–526, Jul. 2010.
[26] H. Kato, M. Fujimaki, T. Noma, and Y. Ohki, "Photo-induced refractive index change in hydrogenated amorphous silicon oxynitride," *J. Appl. Phys.*, vol. 91, no. 10 I, pp. 6350–6353, May 2002.
[27] C. Fiori and R. Devine, "Ultraviolet irradiation induced compaction and photoetching in amorphous, thermal SiO_2," *Proc. Mater. Res. Soc. Symp.*, vol. 61, pp. 187–195, Feb. 1986.
[28] J. Wang *et al.*, "Design of a dual-mode graphene-on-microring resonator for optical gas sensing," *IEEE Access*, vol. 9, pp. 56 479–56 485, 2021.